



Exploring Diverse Modeling Schemes for Runoff Prediction: An Application to 544 Basins in China

3 Yiqian Hu^a, Heng Li^a, Chunxiao Zhang^{a,b,*}, Dingtao Shen^{c,d}, Bingli Xu^e, Min Chen^{f,g,h},
4 Wenhao Chu^a, Rongrong Liⁱ

⁵ ^aSchool of Information Engineering, China University of Geosciences in Beijing, Beijing, China.

⁶ ^bObservation and Research Station of Beijing Fangshan Comprehensive Exploration, Ministry of
⁷ Natural Resources, Beijing, China.

^c Key Laboratory for Geographical Process Analysis & Simulation of Hubei Province, Central China Normal University, 430079, Wuhan, China.

10 ^dCollege of Urban and Environmental Sciences, Central China Normal University, 430079,
11 Wuhan, China.

¹² ¹³ ^e Department of Information and Communication, Academy of Army Armored Forces, Beijing, China.

^f Key Laboratory of Virtual Geographic Environment (Ministry of Education of PRC), Nanjing Normal University, Nanjing, Jiangsu, China.

¹⁶ ^g International Research Center of Big Data for Sustainable Development Goals, Beijing, China.

¹⁷ ^h Jiangsu Center for Collaborative Innovation in Geographical Information Resource
18 Development and Application, Nanjing, Jiangsu, China

ⁱ Institute of Space and Earth Information Science, The Chinese University of Hong Kong, Shatin, New Territories, Hong Kong, China.

21 *Correspondence to: C. Zhang (zcx@cugb.edu.cn)

22 **Key words:** Large-sample hydrological datasets; Deep Learning; LSTM model; Hybrid
23 Modeling; Basin runoff

24 **Abstract**

25 Hydrological modeling plays a key role in water resource management and flood forecasting.

26 However, in China with diverse geography and complex climate types, a systematic evaluation of

27 different modeling schemes for large-sample hydrological datasets is still lacking. This study

For more information, contact the U.S. Environmental Protection Agency (EPA) at 1-800-424-4344 or visit the website at www.epa.gov.

²⁰ For example, and by extension, I evaluated the appropriateness of proposed tariff models (2005), using

short-term memory (STM) models, and hybrid modeling methods. The results demonstrated: (1)

³¹ The accuracy of meteorological data critically impacts the prediction performance of hydrological



32 models. High-quality precipitation data enables the model to better simulate the runoff generation
33 process in the basin, thereby improving prediction accuracy. (2) The hybrid modeling method
34 possesses regional modeling capabilities comparable to those of LSTM model. It also demonstrates
35 strong generalization capabilities. In predicting ungauged basins, the hybrid model exhibits greater
36 stability than the LSTM model. (3) Among the two hybrid modeling methods, the differentiable
37 hybrid modeling scheme offers a deeper understanding and simulation of hydrological processes,
38 along with the ability to output unobserved intermediate hydrological variables, compared to the
39 alternative hybrid modeling schemes. Its prediction results are more consistent with the water
40 balance of the basin. The research results provide a systematic analysis for evaluating the
41 applicability of different hydrological modeling methods in 544 basins in China, offering
42 important guidance for the selection and optimization of future hydrological models.

43 **1. Introduction**

44 **1.1 Challenges in hydrological modeling for China's basins**

45 Global water resources management and hydrological process simulation play a key role in
46 responding to climate change and human activity pressures (Devitt et al., 2023). Accurate
47 hydrological modeling can provide a basis for scientific decision-making for sustainable water
48 resources management, prediction of extreme events, and protection of natural ecosystems (Hoy,
49 2017; Satoh et al., 2022). Among many hydrological variables, daily runoff is particularly widely
50 used. For example, understanding flow patterns (Brunner et al., 2020), efficient water resources
51 management (Patle and Sharma, 2023), reservoir operation and flood prediction (Mangukiya and
52 Sharma, 2025; Mangukiya and Yadav, 2022). However, with the increasing complexity and
53 uncertainty of basin hydrological processes, the applicability and predictive ability of traditional



54 process-based models (PBMs) in practical applications face many challenges, such as insufficient
55 data and complex parameterization.

56 China is located in a densely populated area in East Asia. The rational management of water
57 resources is crucial to economic and social development. Therefore, the role of hydrological
58 modeling in decision support systems has become increasingly prominent (Yin et al., 2018).
59 However, the diversity of topography and the complexity of climate result in significant variations
60 in hydrological processes between basins. This has led to the fact that hydrological models based
61 on physical processes have only achieved certain success in predicting runoff in some basins. For
62 example, Zhang et al. (2024) used the Xin'an jiang model to predict the runoff in the Suihe and
63 Zuohe River basins, and X. Liu et al. (2022) integrated the VIC, Xin'an jiang, and DTVGM models
64 for the Ganjiang River basin. Such models often produce deviations due to insufficient data,
65 structural design defects, or improper parameterization schemes (Dembélé et al., 2020; Herrera et
66 al., 2022; Koch et al., 2016; Silvestro et al., 2015), making it difficult to accurately capture the
67 complex hydrological behavior of the basin. At the same time, with the large-scale growth and
68 sharing of basin data sets, the development of deep learning technology worldwide has provided
69 new tools for hydrological modeling. Especially under the condition of sufficient data, deep
70 learning models such as long short-term memory (LSTM) networks can effectively capture
71 complex nonlinear relationships and provide high-precision predictions by learning large-sample
72 hydrological datasets. However, the applicability and predictive ability of deep learning methods
73 in China's complex hydrological environment have not been fully verified. Hydrological modeling
74 based on a large-sample hydrological dataset whose basins covering various river systems and
75 climate regions in China can provide a relatively clear benchmark. This benchmark can assist in



76 improving relevant hydrological models to solve the runoff prediction problem in China and
77 catchments with similar basin conditions.

78 1.2 Hydrological modeling methods

79 For runoff prediction, existing hydrological modeling methods primarily include process-
80 based models, deep learning models, and hybrid modeling methods that couple the two. Process-
81 based models focus on the physical mechanisms of hydrological processes, provide theoretical
82 support and interpretability, and are particularly suitable for explicitly describing the dynamic
83 hydrological behavior of a basin. However, this type of model emphasizes the uniqueness of
84 hydrological processes and shows that it is impossible to effectively solve different hydrological
85 processes in different basins with a unified approach (Blöschl et al., 2019). Even when used to
86 model hydrology for a single basin, such models typically require a substantial amount of high-
87 quality input data and involve a degree of subjectivity and complexity in the parameterization
88 process. This significantly impacts their applicability and accuracy.

89 In contrast, deep learning models, such as long short-term memory networks (LSTM), learn
90 the dynamic characteristics of basin hydrological processes through historical data, can effectively
91 capture nonlinear relationships, and do not need to rely on precise physical parameters as PBMs.
92 LSTM has attracted great interest in the field of hydrology, and has shown high prediction accuracy
93 and stability in predicting various hydrological variables, including soil moisture (Fang et al., 2017;
94 J. Liu et al., 2022; O. and Orth, 2021), runoff (Feng et al., 2020; Kratzert et al., 2019a), river
95 temperature (Qiu et al., 2021; Rahmani et al., 2023), and dissolved oxygen (Kim et al., 2021; Zhi
96 et al., 2021). This type of model excels in data collaboration (Fang et al., 2022) and therefore
97 thrives in big data environments (Kratzert et al., 2019a; Tsai et al., 2021). This type of model
98 performs well in data-driven collaboration and thrives in big data environments. However, deep



99 learning (DL) methods are not without limitations. On one hand, they may struggle with poor
100 extrapolation ability in the absence of physical constraints, which can limit the model's
101 generalization capability when confronted with unknown climate conditions or long-term
102 predictions, potentially resulting in increased prediction errors and even physically unreasonable
103 results. On the other hand, compared to PBMs that offer clear explanations of physical mechanisms,
104 the predictive results of DL lack interpretability. The variable relationships represented by DL may
105 rely on statistical correlations present in the data rather than true physical causal relationships,
106 which affects its applicability under varying hydrological conditions.

107 To address the limitations of the two aforementioned modeling approaches, hybrid modeling
108 methods have been proposed (Konapala et al., 2020; Willard et al., 2021). The integration of deep
109 learning models and process-based models (PBMs), along with the development of hybrid systems,
110 has been recognized as a promising method for effectively enhancing runoff prediction (Slater et
111 al., 2023). This modeling scheme not only retains the theoretical foundation and interpretability of
112 PBMs but also leverages the robust data fitting capabilities of DL. Common hybrid schemes
113 currently include alternative hybrid modeling scheme and differentiable hybrid modeling scheme.

114 Alternative hybrid modeling scheme commonly employs DL as a post-processing tool to
115 adjust the discrepancies between PBM outputs and actual observations by utilizing PBM outputs
116 as additional input features. For instance, runoff, soil moisture, and snow cover are used as inputs
117 to DL (Amendola et al., 2020; Frame et al., 2021; Wang et al., 2023). Such schemes have been
118 tested in various regions (Cho and Kim, 2022; Shen et al., 2022). DL is trained in a supervised
119 manner, involving only minor modifications to the existing PBMs, which allows for the
120 preservation of valuable physical knowledge inherent in the PBM.



121 Differentiable hybrid modeling scheme is made possible by the emergence of automatic
122 differentiation (auto-diff) technology (Baydin et al., 2018). Automatic differentiation technology
123 calculates gradients automatically through the chain rule, thus avoiding the trouble of manually
124 deriving derivatives and expediting the computation of complex gradients in deep neural networks.
125 This technological advancement addresses the challenge of combining DL with PBMs and
126 significantly enhances the integration of deep learning models into process-based models.
127 Specifically, this hybrid modeling approach neuralizes the process-based model and adjusts model
128 parameters by back propagating gradients based on daily prediction results. This method retains
129 the interpretability of the process model while improving prediction accuracy through deep
130 learning. Additionally, within this unified differentiable architecture, neural networks can
131 selectively replace inaccurate process representations and parameterizations found in process-
132 based models. Due to the innovative nature of this approach, it has garnered significant attention
133 from researchers and has led to the development of multiple variants and adaptations (Frame et al.,
134 2021; Höge et al., 2022; Jiang et al., 2020; Li et al., 2023).

135 1.3 Research gap and study objectives

136 There remains a gap in research regarding the applicability and performance comparison of
137 various hydrological modeling methods in China basins. This highlights a notable research deficit
138 in the field of hydrological modeling for large-sample hydrological datasets of China. Although
139 some scholars have explored different modeling approaches and conducted theoretical analyses
140 and empirical studies, the applicability and predictive capabilities of existing models still require
141 systematic evaluation, especially in the context of China's complex hydrological environment.
142 Specifically, several issues persist in the current research: (1) Comparative studies primarily focus
143 on specific river basins or small sample datasets. For instance, the studies conducted by Wu et al.



144 (2024), Dong et al. (2024), and Xu et al. (2023) centered on small-scale river basins, namely the
145 Weihe River, Lancang River, and Yellow River, respectively. The lack of systematic evaluation
146 across large-sample hydrological datasets limits the feasibility of model promotion and application.
147 Therefore, a systematic evaluation based on large-sample hydrological datasets can not only
148 enhance the generalization ability of the model but also provide a more reliable reference for
149 hydrological predictions nationwide. (2) The guiding principles for model selection in basins with
150 different climatic and attribute characteristics are not yet clear, leading to a lack of relevance in
151 practical applications and difficulty in identifying the optimal modeling methods. In-depth
152 research is needed on the adaptability of different hydrological models in various basin
153 environments, which will help improve modeling efficiency and enhance the stability of
154 predictions. (3) Existing research on the application effects of hybrid modeling methods in China
155 basins, along with their comparative analysis with single models, remains relatively insufficient,
156 resulting in a lack of comprehensive understanding of the relative advantages of different hybrid
157 modeling methods. This limits the further development and optimization of hybrid modeling
158 methods in hydrological prediction. A systematic evaluation of the performance of hybrid
159 modeling methods can not only reveal their potential advantages over traditional methods but also
160 provide directions for future model improvements, offering more accurate and reliable tools for
161 simulating and predicting complex hydrological systems.

162 To address these issues—namely, the limited large-sample studies, unclear model selection
163 guidelines, and insufficient analysis of hybrid models—this study systematically evaluates the
164 applicability of three common hydrological modeling approaches using a comprehensive large-
165 sample hydrological dataset for China. By comparing and analyzing the performance of different
166 models in daily runoff prediction, the study seeks to provide scientific guidance for the selection



167 and application of hydrological models. Specifically, the dataset encompasses 544 basins across
168 nine river systems and seven climate regions in China. It integrates multiple data sources, including
169 remote sensing products and reanalysis data, to relatively accurately describe basin attributes and
170 meteorological characteristics. For each basin, the dataset includes vector boundaries and time
171 series data. The static attribute dataset consists of 6 categories and 15 types. Hydrological and
172 climate attributes are derived by calculating relevant indices from the aforementioned
173 meteorological data, while topographical, soil, vegetation, and geological characteristics are
174 extracted from publicly available global datasets. The hydrological models evaluated in this study
175 include: process-based models (EXP-HYDRO model, Xin'an jiang model), deep learning models
176 (LSTM), alternative hybrid hydrological models (EXP-IN-LSTM, XAJ-IN-LSTM), and
177 differentiable hybrid hydrological models (EXP-dPL, XAJ-dPL). To ensure a fair evaluation, the
178 training periods, testing periods, and the prediction in ungauged basins (PUB, Hrachowitz et al.,
179 2013; Sivapalan et al., 2003) scheme for all models were consistent. In addition to prediction
180 performance, this study also assessed the water balance of each basin using the prediction results
181 of different models. Based on this work, the study not only reveals the applicability of different
182 models in China's basins but also fills the gap in existing research on model comparison in large-
183 sample hydrological datasets and complex basin environments. Furthermore, it provides a
184 performance benchmark and guidance for the selection and improvement of hydrological modeling
185 methods in China in the future.

186



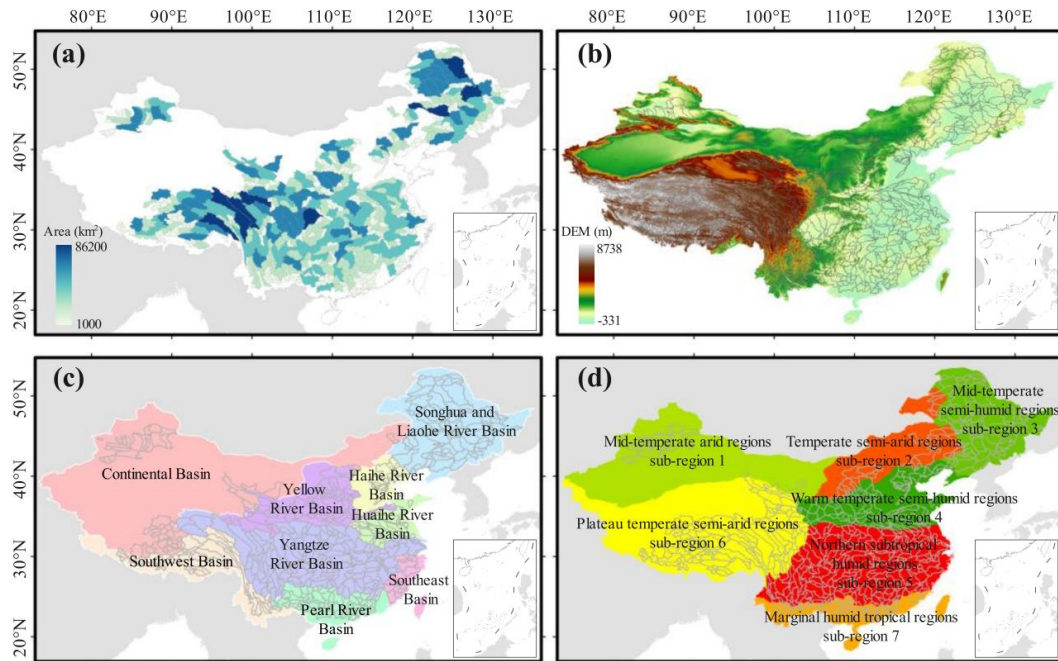
187 **2. Data**

188 **2.1 Study Areas**

189 In China, obtaining a datasets for Large-scale hydrological studies is challenging for two
190 main reasons. Firstly, accurate daily runoff observation data often needs to be kept confidential.
191 Secondly, the start and end times, as well as the quality of data from hydrological observation
192 stations across different regions, can vary significantly. Additionally, the diverse topography and
193 climate conditions in China mean that some watersheds lack essential meteorological and
194 hydrological observation stations (Meng et al., 2017). The primary goal of this study is not to
195 provide a reliable hydrological dataset. Instead, the basic requirement for the dataset is to ensure
196 that the catchment areas encompass a range of climatic and topographic conditions found across
197 China. To meet these requirements, global river network data (Lehner et al., 2008) and DEM
198 elevation data were utilized to delineate the basin vector boundaries. The outlet locations of each
199 catchment (see Figure S1 in Supplementary Materials) were determined using the D8 flow
200 direction scheme. Furthermore, to facilitate the extraction of meteorological forcing data, basins
201 smaller than 1000 km² were excluded from the analysis. Ultimately, the vector boundaries of 544
202 basins were delineated, as shown in Figure 1(a). These 544 basins represent a variety of terrains—
203 including plateaus, plains, and mountains—with average altitudes ranging from 0 to 5000 m. The
204 catchment areas included in this dataset span various types of basins within China's nine river
205 systems (Figure 1(c)) and seven climate regions (Figure 1(d)). Detailed information regarding each
206 river system and climate zone is presented in Table S1 and Table S2 of Supplementary Materials.



207



208

209 **Figure 1. Spatial distribution of 544 basins.** Basin boundaries (a) and areas (b) of the 544
210 basins included in this study. The six defined macro-zones are indicated in blue and purple
211 arrows. (b) and (d) are the divisions of China's nine river systems and seven climate regions,
212 respectively. (The map of China used in this study is from <https://www.tianditu.gov.cn/>.)

213 **2.2 Meteorological forcing and Runoff**

214 The meteorological data used in this study are sourced from the ERA5 (Hersbach et al.,
215 2020) and CN05.1 datasets (Gao et al., 2013). The meteorological forcing elements and their units
216 provided by these datasets are shown in Table 1. We selected these two datasets to extract basin-
217 scale meteorological elements based on the following considerations: (1) ERA5 dataset: Although
218 previous studies (Jiao et al., 2021; Liu et al., 2024) have demonstrated that the meteorological data
219 from ERA5 exhibit certain deviations in Asia, the ERA5 dataset still offers significant advantages.



220 It not only provides a wide variety of meteorological element types but also has an extensive daily
221 meteorological data time span, ensuring dataset completeness. (2) CN05.1 dataset: This dataset is
222 interpolated from observational data collected from over 2,400 meteorological stations across
223 China. Therefore, it can relatively accurately characterize the trends in meteorological changes in
224 the country and offers high spatial resolution and applicability. Utilizing global-scale
225 meteorological data (such as ERA5) alongside more precise meteorological data for specific
226 research areas (such as CN05.1) to evaluate the applicability of different hydrological models can
227 not only enhance the robustness of the evaluation results but also help to verify the differences and
228 applicability of various meteorological data in hydrological predictions.

229 **Table 1** Meteorological forcings data for 544 basins.

Variable name	Description	Unit
total_precipitation_sum	Average daily precipitation	m
temperature_2m	2 m daily mean air temperature	K
potential_evaporation_sum	Total potential evapotranspiration	m
surface_pressure	Near-surface daily average	Pa
surface_solar_radiation_downwards_sum	Short-wave radiation	J/m ²

230 The runoff data provided by the originates from VIC-CN05.1 dataset (Miao and Wang, 2020),
231 which is consistent with the total runoff simulated by the Global Runoff Data Center
232 (UNH/GRDC). Due to the high confidentiality surrounding China's runoff observation data, the
233 number of basins with available runoff data is limited, and the start and end times of the runoff
234 time series vary among different basins. Relying solely on available observational data for
235 calibration may lead to systematic deviations in the runoff data across all basins. The daily runoff
236 time series of each basin outlet were obtained. In order to verify the feasibility of this method, the
237 daily runoff time series of 15 basin outlets with runoff observation data and the runoff hydrograph



238 of actual observation data are shown in Supplementary Figure S2. It can be seen that although it
239 has not been strictly calibrated, the daily runoff time series extracted using the above method can
240 basically reflect the actual runoff change trend of the basin. The aim of this study is not to provide
241 a highly precise basin hydrological dataset but to construct a relatively comprehensive large-
242 sample dataset encompassing meteorological, hydrological, and attribute data for basins across
243 different topographic and climatic regions of China.

244 **2.3 Static catchment attributes**

245 When performing regional modeling, the static attributes of the basin are used as inputs to
246 the model, facilitating the model's ability to learn and extract information related to rainfall-runoff
247 behavior while distinguishing between different basins. This enables the model to interpret the
248 unique characteristics of each basin, thereby improving the accuracy of runoff predictions, as
249 demonstrated by Kratzert et al. (2019b). Therefore, in addition to extracting daily meteorological
250 forcing and runoff data for each basin, the dataset used in this study also includes static basin
251 attribute data. This dataset comprises 15 attributes categorized into six groups: meteorology,
252 hydrology, topography, soil, vegetation, and geology. Among these, meteorological and
253 hydrological attributes are calculated based on the meteorological and runoff time series of each
254 basin. Other static attribute data are derived from global data products based on the vector
255 boundaries of each basin. The abbreviations, meanings, and sources of each static attribute are
256 presented in Table 2. While existing large-sample hydrological datasets (such as CAMELS (Addor
257 et al., 2017) and Caravan (Kratzert et al., 2023)) offer a richer variety of static attributes, our
258 research goal is not to pursue dataset completeness. Instead, we aim to utilize relatively available
259 datasets to evaluate the performance of different models in China. The six categories of static
260 attributes broadly cover the primary factors affecting the hydrological behavior of the basin.



261 Among them, meteorological and hydrological attributes have the most direct and significant
262 impact on runoff, while topography, soil, vegetation, and other attributes can help model to
263 enhance the understanding of basin characteristics from the perspectives of spatial distribution and
264 hydrological processes. Additionally, these static attributes can be obtained through global data
265 products and basin vector boundary calculations, reducing reliance on region-specific data.

266 **Table 2** Static basin attributes data for 544 basins.

Variable name	Description	Unit	Source
area	Basin area	km ²	This study
srf topo	Surface (rock + ice) elevation	m	Amante and Eakins (2009)
slope_avg	Mean subgrid slope (inner slope)	m/m	Amante and Eakins (2009)
wcap	Maximum soil water capacity	Kg/m ²	Hagemann and Stacke (2015)
wava	Plant available water	Kg/m ²	Hagemann and Stacke (2015)
fveg	Fractional vegetation cover climatology relative to LSM	/	Hagemann (2002)
lai	Leaf area index	m ² /m ²	Hagemann (2002)
p_mean	Mean daily precipitation	m	This study
pet_mean	Mean daily potential evapotranspiration	m	This study
aridity	Ratio of Mean PET to Mean Precipitation	-	This study
frac_snow	Fraction of precipitation falling on days with temp < 0 °C	-	This study
high_prec_freq	Frequency of days with $\leq 5 \times$ mean daily precipitation	-	This study
high_prec_dur	Average duration of high precipitation events	-	This study
low_prec_freq	(number of consecutive days with $\leq 5 \times$ mean daily precipitation)	-	
low_prec_freq	Frequency of dry days (< 1 mm/day)	-	This study
low_prec_dur	Average duration of dry periods	-	This study
	(number of consecutive days with precipitation < 1 mm/day)		

267 To facilitate reference and application by researchers in other regions, we have made the
268 global data products used and the code for extracting watershed attributes publicly available. We
269 hope this will enhance the transparency and reproducibility of our research, making it easier for
270 researchers in other regions to replicate and expand upon our methods.

271 **3. Methodology**

272 **3.1 Experimental design**

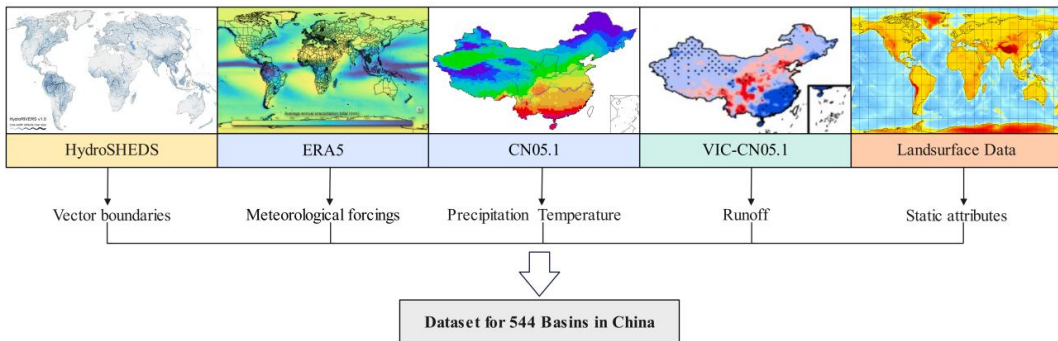
273 When extracting data based on the basin vector boundary, it is essential to ensure the
274 consistency of the time span for both runoff and meteorological data. To eliminate potential



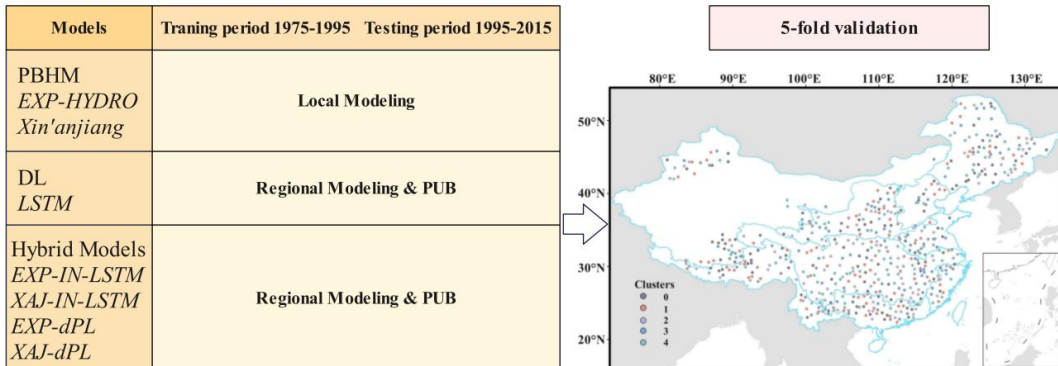
275 deviations caused by differing start and end times across various data sources, the time range for
276 all data is standardized from October 1, 1975, to September 30, 2015. For different hydrological
277 models, the training and testing periods are uniformly established: the training period spans from
278 October 1, 1975, to September 30, 1995, while the testing period extends from October 1, 1995,
279 to September 30, 2015. This consistent division facilitates an accurate evaluation of the fitting and
280 predictive capabilities of different models concerning the runoff process. Furthermore, to further
281 assess the generalization performance of the models, a five-fold cross-validation method is
282 implemented. Specifically, the 544 basins are divided into five relatively even clusters (with each
283 cluster containing either 109 or 108 basins, as shown in Figure 2). The validation process is as
284 follows: the model is trained using the training period data from the basins in nine of the clusters,
285 and its performance is validated on the test period data from the remaining cluster. This operation
286 is repeated in a loop, with each iteration designating a different cluster as the ungauged basin,
287 thereby allowing for the evaluation of the predictive performance of each basin treated as an
288 ungauged basin.



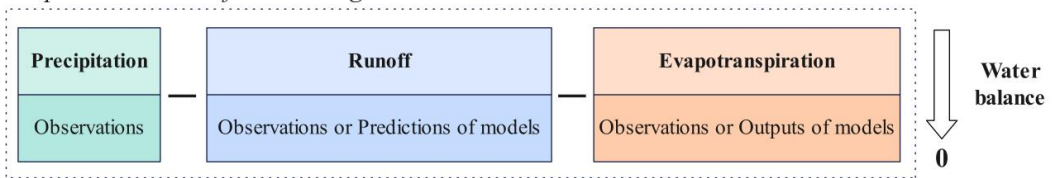
Step 1 Data preprocessing



Step 2 Model Performance Evaluation



Step 3 Evaluation of water budget closure





297 can output include snow accumulation, snowmelt, evapotranspiration, soil moisture, and runoff.

298 The calibration of the model is governed by six physically meaningful hydrological parameters

299 (the specific meanings of these parameters are provided in Table S3 of Supplementary Materials).

300 The original version of the Xin'anjiang model is a rainfall-runoff model designed for hydrological

301 forecasting in humid and semi-humid regions (Ren-Jun, 1992). To enhance the model's

302 applicability under complex climatic conditions, this study employs a simplified version of the

303 Xin'anjiang model, as depicted in Figure 3(b). The simplified model retains four main subprocesses

304 from the original Xin'anjiang model: evapotranspiration, runoff generation, runoff separation, and

305 runoff routing. While the original model considered the impact of impervious surfaces on runoff,

306 this aspect has been simplified in the current study to better align with research needs and data

307 characteristics. Nevertheless, the model retains its core hydrological processes and can effectively

308 simulate the hydrological behavior of the basin. The evapotranspiration module accounts for

309 evaporation from three layers of soil (upper, lower, and deep layers) and calculates the

310 evapotranspiration for each layer using an empirically defined formula based on the soil moisture

311 content and evapotranspiration rates. The runoff generation module simulates moisture

312 distribution and initiates runoff formation. The generated runoffs are subsequently separated into

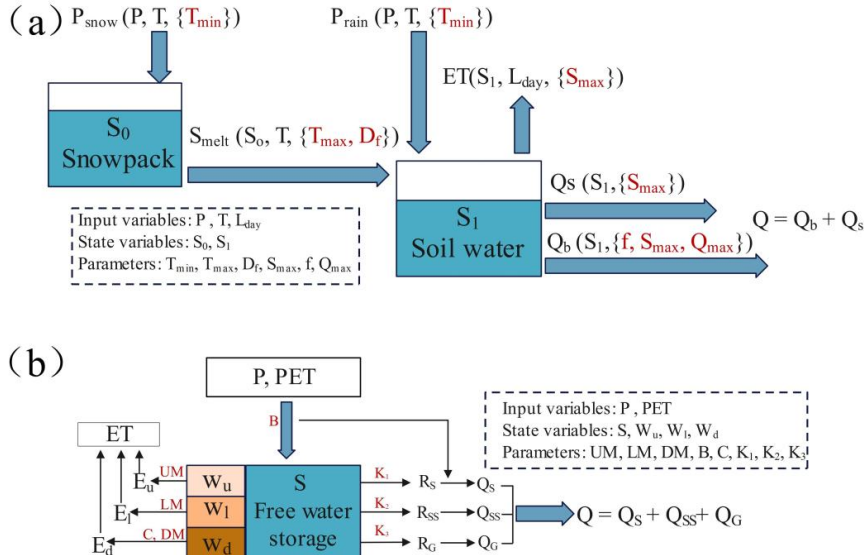
313 surface runoff, convergence, and groundwater by the runoff separation module based on free water

314 storage. Finally, the runoff routing module directs the water flow to the basin outlet for surface

315 runoff and into linear reservoirs for groundwater flow. A total of 8 hydrological parameters are

316 integrated into the adjusted Xin'anjiang model. Further details can be found in Table S4 of

317 Supplementary Materials.



318

319 **Figure 3. The structure of the EXP-HYDRO (a) and adapted Xin'anjiang model (b).**

320 3.3 Deep learning model

321 With the continuous advancement of deep learning technology, its applications in the field of
 322 hydrology are also expanding. This study utilizes the classic LSTM model as a representation of a
 323 purely data-driven approach. LSTM, a type of recurrent neural network (RNN), was first proposed
 324 by Hochreiter and Schmidhuber (1997). Kratzert et al. (2018) applied the LSTM model to rainfall-
 325 runoff modeling. The specific structure of the LSTM model can be described by the following
 326 equations:

$$i[t] = \sigma(W_i x[t] + U_i h[t-1] + b_i) \quad (1)$$

$$f[t] = \sigma(W_f x[t] + U_f h[t-1] + b_f) \quad (2)$$

$$g[t] = \tanh(W_g x[t] + U_g h[t-1] + b_g) \quad (3)$$

$$o[t] = \sigma(W_o x[t] + U_o h[t-1] + b_o) \quad (4)$$

$$c[t] = f[t] \odot c[t-1] + i[t] \odot g[t] \quad (5)$$

$$h[t] = o[t] \odot \tanh(c[t]) \quad (6)$$



333 where $i[t]$, $f[t]$, and $o[t]$ are the input, forget, and output gates, respectively, $g[t]$ is the cell input,
334 $x[t]$ is the network input at time step t ($1 \leq t \leq T$), and $h[t-1]$ is the recurrent input $c[t-1]$ of the
335 cell state at the previous time step. $\sigma(\cdot)$ is the sigmoid activation function, $\tanh(\cdot)$ is the hyperbolic
336 tangent function, and \odot is an element-wise multiplication. Intuitively, the cell state ($c[t]$)
337 characterizes the memory of the system. These are modified by a combination of (i) the forget gate
338 ($f[t]$) and (ii) the input gate ($i[t]$) and the cell update ($g[t]$). Ultimately, the output gate ($o[t]$)
339 controls the flow of information from the state to the model output.

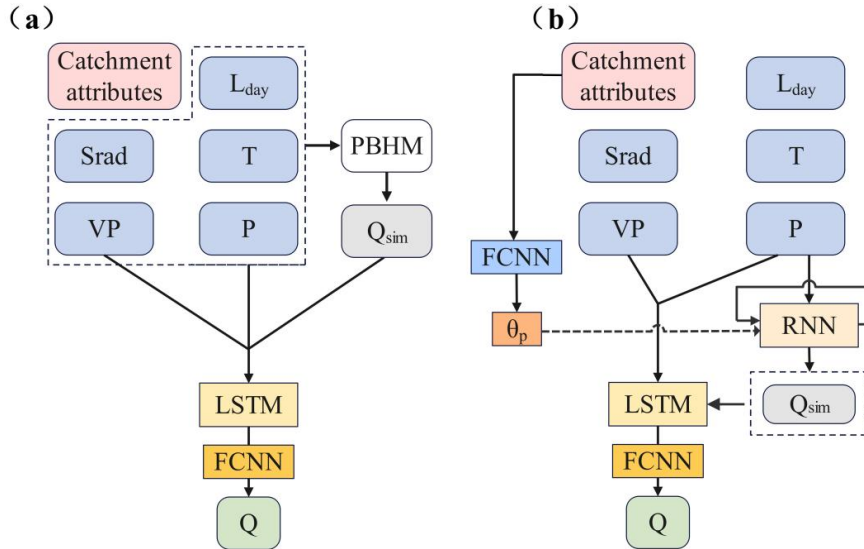
340 The LSTM model architecture used in this study to predict daily runoff in China consists of
341 a hidden layer with 256 hidden units. The regional LSTM model uses 20 input features: 5
342 meteorological forcings and 15 static basin attributes. All input data are normalized before training.
343 Additionally, to ensure that the model learns the temporal variation of runoff while taking into
344 account training efficiency, we input a sequence of 365 days into the network for each batch size
345 and use a sliding window of 31 days to learn all sequences. Furthermore, to understand the impact
346 of basin attributes on runoff, the operation of basin attributes across different basins also follows
347 the aforementioned sliding window learning rules. The LSTM employs the Adaptive Moment
348 Estimation algorithm (Adam, Kingma and Ba, 2014) to estimate model parameters. The initial
349 learning rate is set to 0.01, and the maximum number of training iterations is set to 150. All the
350 LSTM models are trained using the specified hyperparameters.

351 3.4 The hybrid models

352 Both alternative hybrid modeling and differentiable hybrid modeling schemes are designed
353 to couple the advantages of PBM and DL models. The architectures of the two types of models are
354 shown in Figure 4. PBM represents both the EXP and XAJ models, which are utilized to extract
355 and characterize the physical mechanisms involved in hydrological processes. LSTM serves as



356 either a post-processing tool or a differentiable component, integrating with PBM to create
357 alternative hybrid models and differentiable hybrid models. In the alternative hybrid modeling
358 scheme depicted in Figure 4(a), LSTM functions as a post-processing tool to adjust discrepancies
359 between the PBM outputs and observations. This model's input includes not only the results
360 predicted by PBM but also the input variables of the pure data-driven model, including
361 meteorological forcing and static basin attributes. This approach allows the alternative hybrid
362 modeling method to retain the explanatory power of the physical mechanisms inherent in the
363 process model while leveraging LSTM's capability to effectively capture nonlinear relationships,
364 thereby compensating for the limitations of PBMs in large-sample hydrological datasets and
365 complex basins. In the differentiable hybrid modeling scheme shown in Figure 4(b), discrete
366 ordinary differential equations based on PBM are encoded into standard recurrent neural network
367 (RNN) units, encompassing the water balance law and fundamental hydrological processes.
368 Simultaneously, the neural network acts as a parameterized channel, incorporating static attributes
369 as additional input variables into the overall model framework for joint optimization. This enables
370 the model to dynamically adjust hydrological parameters based on the characteristics of basin
371 attributes, overcoming the traditional physical process models' reliance on fixed parameterization,
372 and adapting to runoff relationships across different basins and climatic conditions.



373

374

Figure 4. The structure of the hybrid hydrological models.

375

Specifically, the hybrid hydrological models developed in this study include four types: (1) a
376 alternative hybrid model that uses EXP-predicted runoff values as an additional input to LSTM
377 (EXP-IN-LSTM); (2) a alternative hybrid model that uses XAJ-predicted runoff values as an
378 additional input to LSTM (XAJ-IN-LSTM); (3) a differentiable hybrid model that retains the EXP
379 structure while incorporating the LSTM network for parameter learning (EXP-dPL); and (4) a
380 differentiable hybrid model that retains the XAJ structure while incorporating the LSTM network
381 for parameter learning (XAJ-dPL). The details for all the hybrid models trained and tested in this
382 study—including input data, training sets, testing sets, and inputs—are presented in Table S5 of
383 Supplementary Materials.

384

4. Results and discussion

385 4.1 Meteorological forcing assessment

386 Figure 5 shows the spatial distribution of average annual precipitation and average daily
387 temperature for each station under different datasets. Overall, although neither of the two



388 meteorological datasets has been corrected using station observation data, their spatial
389 distributions are largely similar. Precipitation exhibits a decreasing trend from the southeastern
390 coast to the northwestern inland areas. Temperature decreases with increasing latitude in the east,
391 and the temperatures in the Qinghai-Tibet Plateau are relatively low due to the influence of altitude
392 and terrain. It should be noted that by observing the frequency distribution curves of the average
393 annual temperature and average daily temperature of 544 basins, it can be seen that the overall
394 temperature distribution in the two datasets is quite similar. However, the distribution of the
395 precipitation data shows significant differences. The precipitation data provided by ERA5 varies
396 greatly between different basins, showing some extremely wet or extremely dry basins, while the
397 precipitation data provided by CN05.1 is relatively uniform across basins.

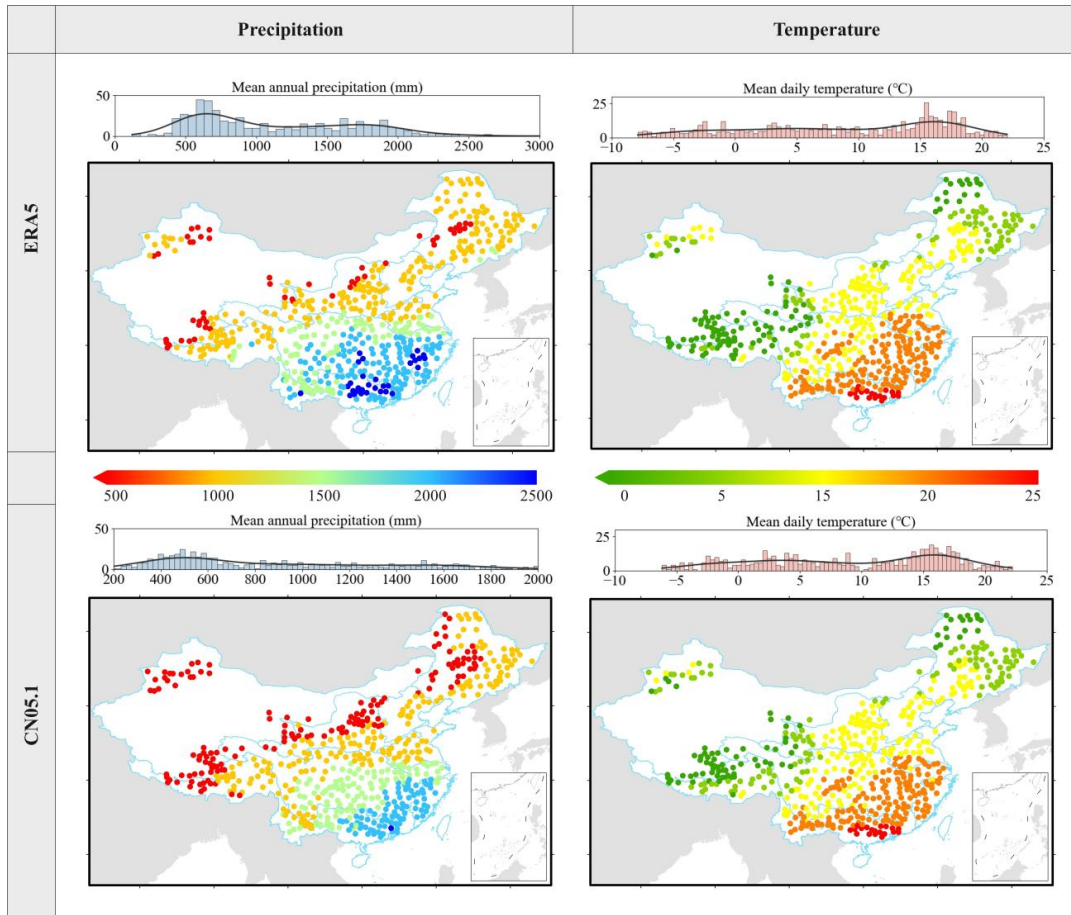


Figure 5. Spatial distribution of precipitation and temperature in 544 basins using ERA5 and CN05.1 Datasets.

In order to further explore the differences and systematic biases in various meteorological datasets, the Budyko framework (Budyko and Miller, 2010) was employed to determine the impact of different precipitation data on the water balance of various basins. This framework links climate with basin runoff and evapotranspiration in a simple and intuitive manner, aiming to facilitate the analysis of how evapotranspiration and runoff in each basin are influenced by available energy and precipitation. Figure 6 shows a scatter plot of the evaporation index (EI, the ratio of annual average evapotranspiration to annual average precipitation) and the drought index. When using the same runoff and evapotranspiration data, the precipitation data provided by ERA5 resulted in more



409 basins (111) violating the water-heat balance. In these relatively humid basins, the relationship
410 between precipitation and evaporation did not adequately satisfy the water-heat balance conditions.
411 In contrast, when using CN05.1 data, fewer basins (12), concentrated in humid basins at medium
412 and high altitudes) violated the water-heat balance. It should be noted that this difference may be
413 related to the quality and processing methods of the data source. On one hand, ERA5 is a global
414 meteorological model, and its precipitation data has not been corrected using station observation
415 data, which may lead to significant deviations. On the other hand, the runoff data product used in
416 this study was simulated by the VIC model, which uses CN05.1 meteorological data. VIC (Liang
417 et al., 1994) is a hydrological model based on physical processes, incorporating the equations of
418 water conservation and energy conservation into its implementation logic to ensure the scientific
419 and physical consistency of the simulation. This results in fewer basins violating the water-heat
420 balance when using CN05.1 precipitation data to validate the Budyko framework. When
421 establishing large-sample hydrological datasets cross different regions, it is necessary to consider
422 the water budget balance at the watershed scale. We recommend that future studies aimed at
423 creating accurate large-sample hydrological datasets in China should consider the water and
424 energy balance of each watershed while fully calibrating each dataset, especially for high-altitude
425 watersheds that are relatively humid.

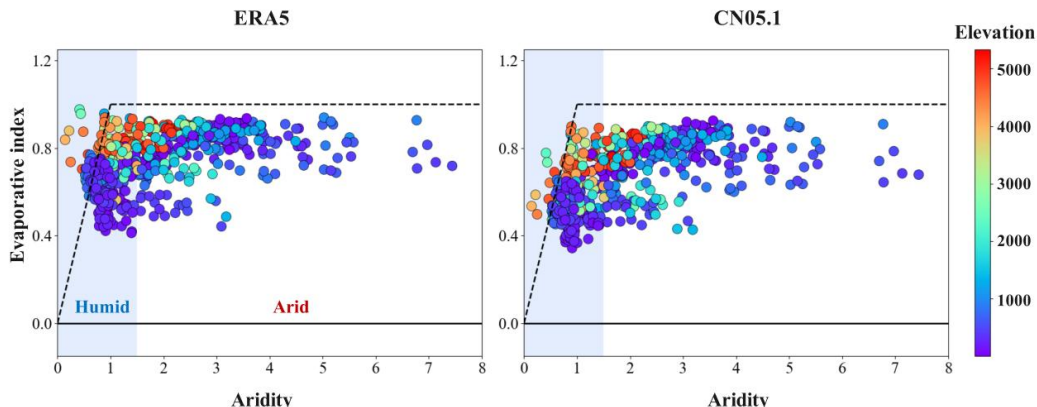
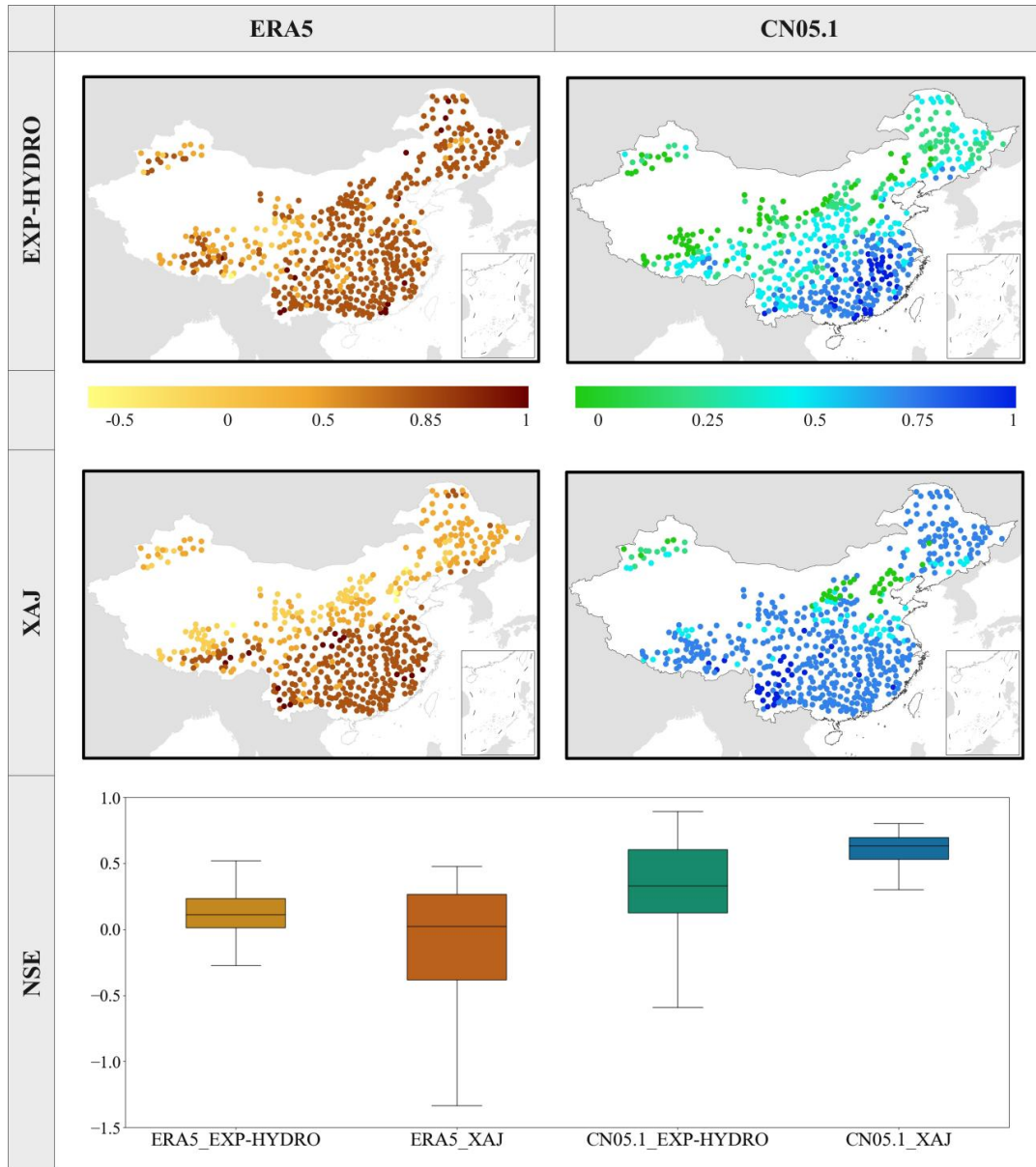


Figure 6. Water balance for 544 basins, illustrated in a Budyko scheme for ERA5 (a) and CN05.1 (b). Markers are coloured by the basin mean elevation.

426 4.2 Performance comparison of process-based models

427 Figure 7 shows the runoff prediction performance of different PBMs for 544 basins. Overall,
428 both the EXP and XAJ models demonstrate greater accuracy in representing the rainfall-runoff
429 relationship for the wetter basins in the southeast compared to the inland basins in the northwest.
430 The prediction skills of both PBMs show significant improvement when using precipitation data
431 from CN05.1 as input, in contrast to using ERA5 precipitation data. Notably, for the XAJ model,
432 the median NSE across the 544 basins reaches 0.63 when using CN05.1 precipitation data.
433

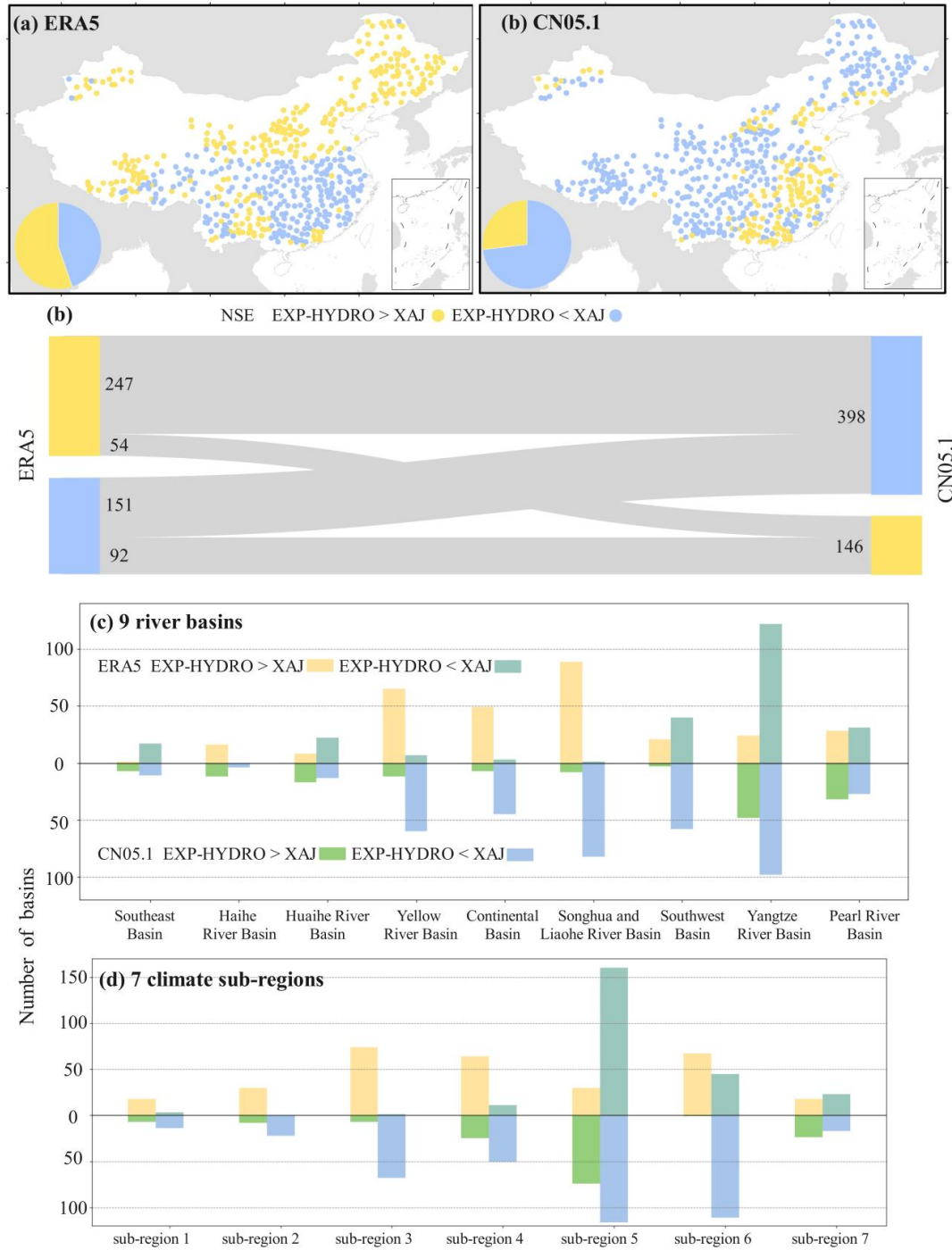


436
437 **Figure 7. Performance of process-based hydrological models during the testing period**
438 **(1995.10.1–2015.9.30). Spatial distributions of the Nash-Sutcliffe efficiency (NSE) for EXP-**
439 **HYDRO model and Xin'anjiang model. The NSE colormap is capped within [0, 1] for**
440 **better visualization.**

441 Furthermore, the specific performance differences of different PBMs in each basin are
442 compared. Figures 8(a) and 8(b) show which PBMs exhibit better prediction performance in each



443 basin under varying precipitation data. In general, the source of precipitation data significantly
444 influences the selection of PBMs for most basins. This means that for the same basin, if the input
445 precipitation data sources differ, the choice of PBM should be adjusted accordingly. Additionally,
446 some basins show consistent selection preferences under the two sets of precipitation data. For
447 instance, in most basins located in the middle and lower reaches of the Yangtze River and the
448 southeastern rivers, which are relatively humid, the XAJ model is a better choice than the EXP
449 model under different precipitation data. Despite the differences in precipitation data, the EXP
450 model consistently outperforms the other models for most basins in the Haihe River system. For
451 nearly half of the basins (247), the EXP model demonstrates superior prediction performance when
452 using ERA5 precipitation data, while the XAJ model performs better with CN05.1 data. This
453 indicates that the applicable PBM for the same basin may change solely due to variations in
454 precipitation data. Thus, in addition to the climatic characteristics of the basin, the accuracy and
455 reliability of meteorological data play a crucial role in determining the prediction performance of
456 PBMs.



457

458

459

Figure 8. Comparison of EXP-HYDRO model and Xin'anjiang model performances in different basins using ERA5 and CN05.1 precipitation data.



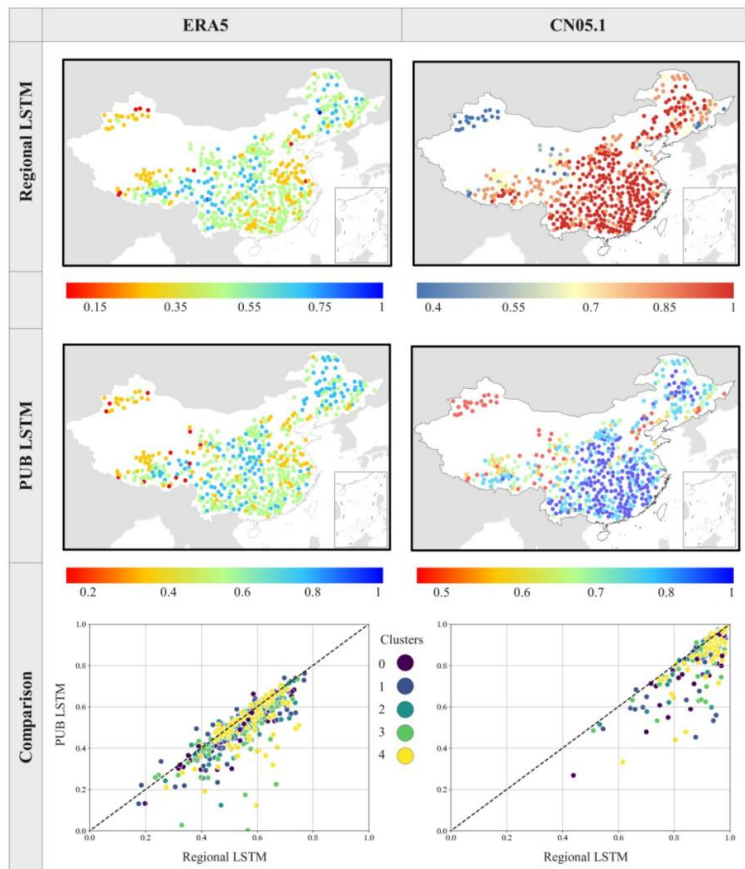
460 4.3 Performance and generalization of LSTM

461 Figure 9 shows the prediction performance of the purely data-driven LSTM model in regional
462 modeling and PUB under different precipitation data sources. Similar to performances in large-
463 sample hydrological datasets of other regions, the LSTM model also demonstrates strong
464 capabilities in handling large amounts of hydrological data and excels in runoff prediction in large-
465 sample hydrological dataset in China. Specifically, when using ERA5 precipitation data, the
466 median NSE of LSTM across 544 basins reaches 0.57 ($\text{NSE} \geq 0.55$ is considered the threshold
467 for good performance (Knoben et al., 2019; Newman et al., 2015)). When using CN05.1
468 precipitation data, the median NSE for LSTM in regional modeling and PUB reached an
469 impressive 0.95 and 0.93, respectively. This phenomenon may be due to the runoff data product
470 used in this study, which is also simulated using CN05.1 data (as described in Section 4.1). The
471 use of CN05.1 precipitation data enables other subsequent models to demonstrate excellent
472 prediction performance, a point that will not be revisited in the following sections.

473 It is worth noting that under different precipitation data, when the PUB of 544 basins was
474 conducted using five-fold cross-validation, the prediction skills were comparable to those of
475 regional modeling. This indicates that the LSTM model also possesses strong generalization ability
476 in China's basins, achieving more accurate hydrological predictions in ungauged basins by learning
477 from hydrological data of other basins. Surprisingly, under the ERA5 precipitation data conditions,
478 the PUB results for some basins outperformed the prediction performance of regional modeling.
479 In theory, regional modeling uses data from all basins for training and is generally regarded as
480 providing superior predictions, especially for individual basins. When a basin's own data is
481 included in the training set, the model is expected to perform better in predicting that basin's runoff.
482 However, as illustrated in the scatter plot at the bottom of Figure 9, there are instances where the



483 PUB performance exceeds that of regional modeling when different precipitation data are used.
484 Notably, under the ERA5 conditions, the number of such basins is higher. This phenomenon may
485 indicate that the ERA5 precipitation data exhibits a certain degree of non-uniformity among
486 different basins (as shown in Figure 5), which affects the effectiveness of regional modeling. The
487 accuracy and spatial consistency of meteorological data jointly determine their impact on the
488 predictive performance of hydrological models. This not only influences the model's
489 representation of hydrological processes but may also significantly shape its generalization
490 performance. Therefore, we suggest that future related studies should comprehensively consider
491 the differences in training samples while also taking into account the accuracy of model input data.



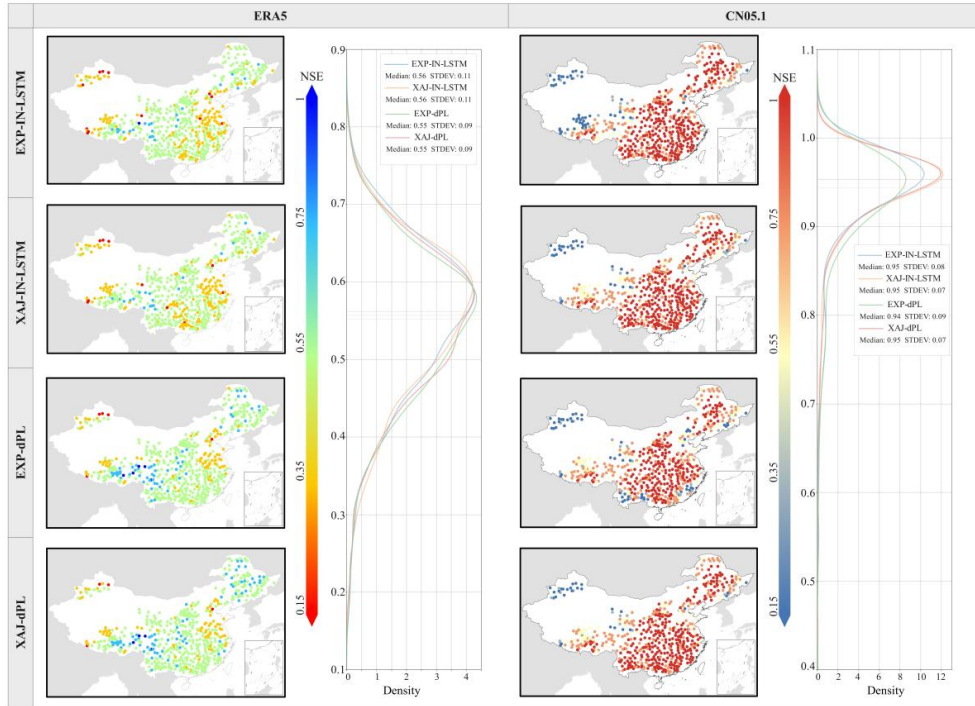
492



493 **Figure 9. LSTM models prediction performances using ERA5 and CN05.1 precipitation**
494 **data.**

495 4.4 Performance and selection of hybrid models

496 Figure 10 shows the prediction performance of four alternative and differentiable hybrid
497 hydrological models for regional modeling across 544 basins. When the model input is based on
498 the CN05.1 dataset, the overall performance of the different hybrid models aligns closely with that
499 of the pure LSTM model, and the spatial distribution characteristics of the NSE across the 544
500 basins are also highly similar. However, when the ERA5 precipitation data is used for regional
501 modeling, the distribution of NSE varies among the basins. Although the median NSE of each
502 hybrid model and the pure LSTM model across the 544 basins is generally consistent, coupling
503 the process-based model (PBM) with LSTM results in a more stable prediction performance across
504 different basins. This improvement may be attributed to the fact that the differentiable hybrid
505 model follows to the law of water balance during the modeling process, avoiding the sacrifice of
506 performance in more challenging basins in order to improve the overall performance across all
507 basins. Therefore, the modeling strategy that couples PBM with deep learning, particularly the
508 differentiable hybrid hydrological model, can not only maintain overall prediction accuracy but
509 also enhance the spatial robustness of the model and balance prediction skills across different
510 basins.



511

512

513

Figure 10. Four hybrid models prediction performances using ERA5 and CN05.1 precipitation data.

514

Further analysis of the specific performance of different basins under various hybrid models

515

is presented in Figure 11 (a) and (b), which show the distribution of the optimal hybrid model for

516

each basin based on two sets of precipitation data. In general, under the two precipitation datasets,

517

CN05.1 and ERA5, the alternative hybrid modeling scheme—where the predicted values of the

518

PBMs are used as an additional input for deep DL—exhibits superior performance across more

519

basins than the differentiable hybrid modeling scheme, which involves parameterizing the process

520

model and coupling it with DL. Although the optimal hybrid model for some basins remains

521

consistent regardless of the precipitation data used as input, for most basins, changes in the input

522

data lead to a shift in the most suitable hybrid model. This phenomenon indicates that the accuracy

523

and reliability of meteorological data significantly influence the selection of hybrid models.



524 Figures 11 (c) and (d) show the distribution of the best hybrid models across various water
525 systems and climate regions. The results indicate that the Yellow River Basin and the Songliao
526 River Basin show a clear preference for alternative hybrid modeling methods. Notably, in the
527 Songliao River Basin (climate region 3), the EXP-INLSTM model outperforms others in a greater
528 number of basins. This may be attributed to the fact that the EXP-HYDRO model includes rain-
529 snow partitioning and snowmelt modules specifically designed to address snow storage, allowing
530 for a more accurate representation of the influence of snow on runoff. Additionally, in climate
531 region 6 (the high-altitude region of the Qinghai-Tibet Plateau), the EXP-dPL model demonstrates
532 strong suitability when using CN05.1 data. This area is influenced by the combined effects of
533 perennial snow and frozen ground, while the high-latitude climate region 3 is primarily impacted
534 by seasonal snow. This distinction indicates that although the hybrid modeling scheme coupling
535 EXP and LSTM generally outperforms the combination of XAJ and LSTM in basins affected by
536 snow storage, further subdivision reveals that different hybrid methods involving EXP and LSTM
537 may be better suited for basins with varying snow characteristics

538 Moreover, the optimal hybrid model for most basins is influenced by the source of
539 meteorological data. In humid regions, such as the middle and lower reaches of the Yangtze River
540 and the Southeastern Rivers, the hybrid models combining XAJ and LSTM generally outperforms
541 the hybrid models of EXP and LSTM across different precipitation datasets. Conversely, in the
542 Haihe River, the EXP and LSTM hybrid model consistently represents the best choice for most
543 basins. In other basins with varying climatic characteristics, the hybrid models of EXP and LSTM
544 demonstrate better predictive performance under ERA5 data, whereas the XAJ and LSTM hybrid
545 model performs better under CN05.1 data. This further confirms the impact of the accuracy and
546 reliability of meteorological data on the selection of hybrid hydrological models.

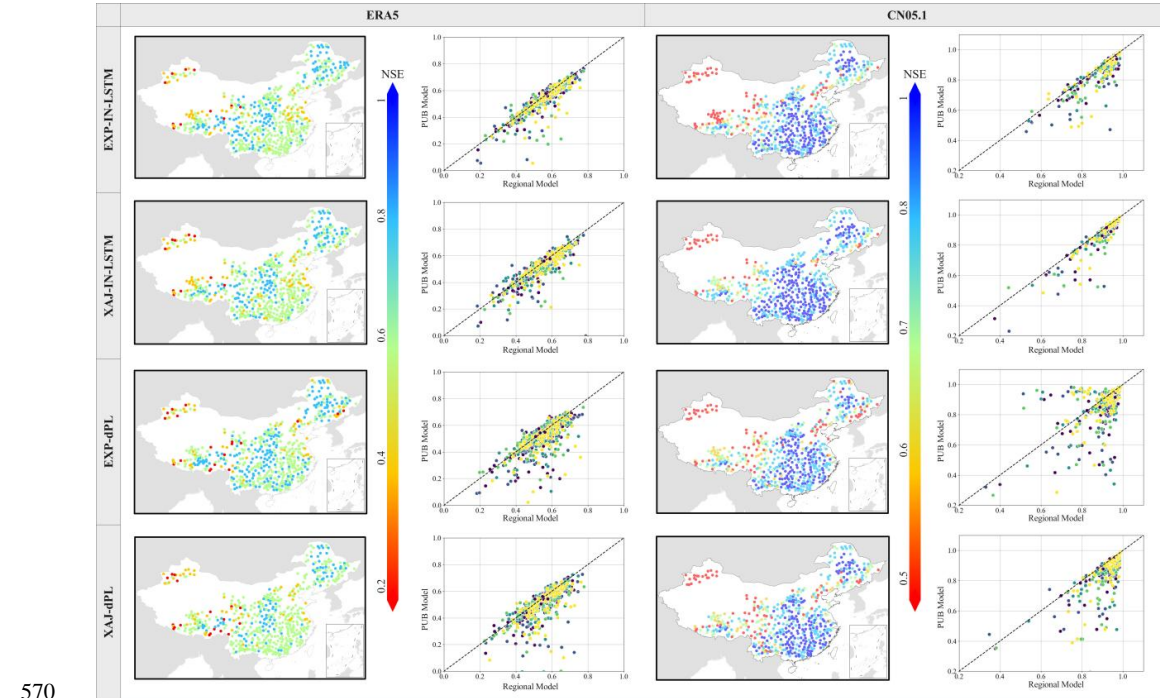




548 **Figure 11. Comparison of hybrid models performances across basins using ERA5 and**
549 **CN05.1 precipitation data.**

550 To evaluate the generalization ability of different hybrid hydrological models, the same PUB
551 scheme for pure LSTM described in Section 4.3 was adopted to conduct 5-fold cross-validation
552 on 544 basins. The prediction performance of each hybrid model, using different precipitation data
553 as input, is shown in Figure 12. Overall, the prediction performance distribution of various hybrid
554 hydrological models across the 544 basins is relatively consistent under the same input data. With
555 ERA5 precipitation data, the hybrid model that performed best in the PUB is EXP-dPL, with a
556 median NSE of 0.55. In contrast, under CN05.1 precipitation data, XAJ-dPL demonstrates the best
557 generalization ability, achieving a median NSE of 0.95. It is worth noting that when different
558 meteorological data are used as input, the differentiable hybrid model exhibits better predictive
559 performance than the alternative hybrid model in the PUB. This indicates that the differentiable
560 modeling scheme can enhance the adaptability and generalization performance of the hybrid model
561 in ungauged basins.

562 The scatter plots in Figure 12 show the comparison of NSE values between regional modeling
563 and PUB for each basin. Under CN05.1 precipitation data, when XAJ-dPL was tested through 5-
564 fold cross-validation, the prediction performance of certain basins exceeded that of regional
565 modeling significantly. This phenomenon indicates that not all basins require their own historical
566 data for training when making hydrological predictions. In some cases, modeling based on the
567 hydrological information from other basins in the region can achieve better prediction results. This
568 further verifies the potential of hybrid modeling strategies, particularly differentiable hybrid
569 modeling methods, in enhancing model extrapolation capabilities and generalization performance.



570

571 **Figure 12. Comparison of PUB performances of four hybrid models.**

572 **4.5 Evaluation of water budget closure**

573 To verify the physical consistency of the prediction results from different models, the water
574 budget closure and water imbalance ratio for 544 basins were calculated during the test period.
575 This study used a adapted long-term water budget for each basin (Tan et al., 2022; Wang et al.,
576 2014) to evaluate the basin water balance closure:

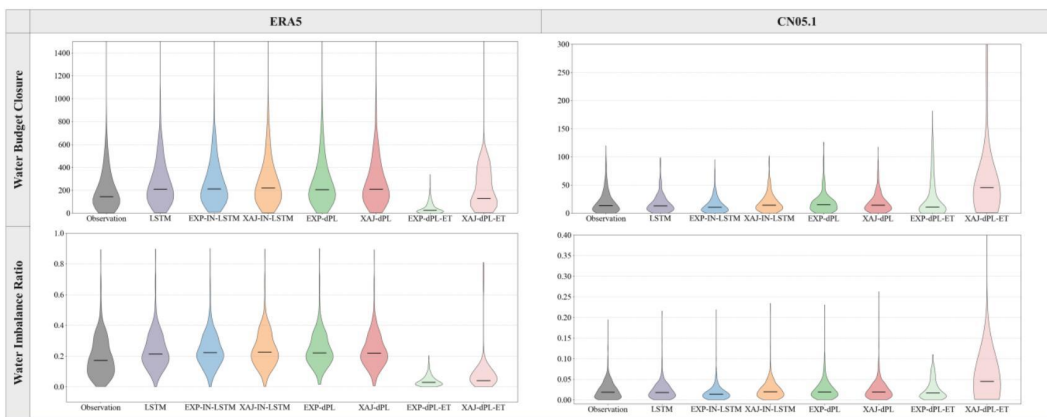
$$|P - ET - Q| = \epsilon \quad (7)$$

577 Where P is precipitation from ERA5 or CN05.1 dataset, ET is evapotranspiration (observations
578 provided by ERA5 or output of differentiable hybrid models), Q is runoff (observations or
579 predictions from different models), and ϵ is the water budget imbalance. The smaller the value of
580 ϵ , the better the water budget balance of the basin.

582 Figure 13 shows the difference of the annual water budget closure (ϵ) and the water imbalance
583 ratio (ϵ/P) for 544 basins among different models. The detailed data sources for runoff and



584 evapotranspiration associated with the various indicators in the figure are provided in Table S6 of
585 Supplementary Materials. The results show that when the simulated runoff from different hybrid
586 models replaces the observed values, the basin's water balance closure does not change
587 significantly. However, when the evapotranspiration data output by EXP-dPL replaces the original
588 ET data, the overall water imbalance across the 544 basins is significantly reduced. This
589 phenomenon indicates that, under the framework of EXP-dPL, the model's runoff output can not
590 only maintain high prediction accuracy but also conform better to the water budget constraint,
591 reflecting good physical consistency. It should be noted that the dataset used in this study has not
592 been strictly calibrated against actual observation sites, which may be one of the reasons why the
593 ET data output by XAJ-dPL caused a deterioration in water balance closure in some basins.
594 Nevertheless, the above results can still prove to a certain extent that the differentiable hybrid
595 modeling method can not only provide high-precision runoff predictions, but also output
596 intermediate hydrological variables that align with hydrological mechanisms. This ensures better
597 compliance with physical constraints while maintaining prediction performance. Therefore, the
598 differentiable hybrid modeling scheme represents a modeling approach that balances both physical
599 consistency and prediction skills.



600



601 **Figure 13. Distribution of annual (a) water budget closure (ϵ) and (b) water imbalance**
602 **ratio (ϵ/P) for all 544 basins during the test period.**

603 **5. Conclusion**

604 This study systematically evaluated the hydrological modeling of a large-sample hydrological
605 dataset for 544 basins in China, analyzed the applicability of multiple hydrological models in
606 complex hydrological environments, and provided a valuable basis for the selection and
607 optimization of future hydrological models. Through a comparison of different hydrological
608 modeling methods, the study reached the following three main conclusions:

609 (1) The accuracy and reliability of meteorological data have a key impact on the predictive
610 performance of hydrological models. For most basins in China, changes in the source of
611 meteorological data may lead to differences in the performance of similar models.

612 Accurate precipitation data can help models better simulate the runoff generation process
613 in the basin, thereby more effectively capturing the hydrological characteristics of the
614 basin. During the selection and application of models, the quality and adaptability of
615 meteorological data are crucial factors that determine the model's predictive capability.

616 (2) The hybrid modeling method shows strong predictive performance and generalization
617 capabilities. In the prediction of ungauged basins, whether using ERA5 or CN05.1
618 precipitation data, the generalization ability of the hybrid modeling method surpasses that
619 of the pure LSTM model. This indicates that the hybrid model is better equipped to adapt
620 to the basins with different hydrological characteristics, providing more stable prediction
621 results. This highlights the advantages of hybrid modeling methods in complex
622 hydrological environments and their robust adaptability across various regions and
623 climatic conditions.



624 (3) Compared with alternative hybrid modeling schemes, the differentiable hybrid modeling
625 scheme achieves a deeper understanding of hydrological processes. Due to the seamless
626 coupling of process-based models, the differentiable hybrid hydrological model can
627 output unobserved intermediate hydrological variables. At the same time, the runoff
628 prediction results of this hybrid modeling scheme are more consistent with the water
629 budget balance at the basin scale, providing more comprehensive and accurate support
630 for hydrological prediction.

631 Although this study provides a relatively systematic evaluation of hydrological modeling in
632 China's basins, the meteorological and runoff data used have not been corrected, which may limit
633 the applicability of the dataset. Future studies should consider using observational data for
634 correction to enhance the dataset's reliability and further improve the accuracy of model
635 predictions. While this study primarily focuses on basins in China, it is hoped that the methods
636 and datasets presented in this research can serve as a reference for other regions lacking
637 observational data and promote similar hydrological modeling efforts worldwide.

638 **Data and Code Availability**

639 The dataset for 544 China basins in this study can be downloaded from
640 [https://github.com/Yq-H47/Catchment-Attributes-and-Meteorology-dataset-for-China-544-
641 basins](https://github.com/Yq-H47/Catchment-Attributes-and-Meteorology-dataset-for-China-544-basins). And the models are available at <https://github.com/Yq-H47>.

642 **Declaration of competing interest**

643 No potential conflict of interest was reported by the authors.

644 **Acknowledgment**

645 This work was supported by the National Natural Science Foundation of China (grant
646 numbers 42371425, 42325107, 42330108).



647 **CRediT authorship contribution statement**

648 **YH:** Conceptualization, Data curation, Formal analysis, Funding acquisition, Investigation,
649 Methodology, Software, Visualization, Writing – original draft. **HL:** Conceptualization, Data
650 curation, Formal analysis, Investigation, Methodology, Software, Validation, Writing – original
651 draft. **CZ:** Conceptualization, Funding acquisition, Investigation, Methodology, Resources,
652 Supervision, Writing – review & editing. **DS:** Funding acquisition, Resources, Supervision,
653 Writing – review & editing. **BX:** Conceptualization, Investigation, Methodology, Resources,
654 Supervision, Writing – review & editing. **MC:** Conceptualization, Funding acquisition,
655 Investigation, Methodology, Resources, Supervision, Writing – review & editing. **WC:** Data
656 curation, Visualization, Writing – original draft. **RL:** Writing – original draft, Writing – review &
657 editing.

658 **References**

- 659 Abadi, M., Agarwal, A., Barham, P., Brevdo, E., Chen, Z., Citro, C., Corrado, G.S., Davis, A.,
660 Dean, J., Devin, M., Ghemawat, S., Goodfellow, I., Harp, A., Irving, G., Isard, M., Jia, Y.,
661 Jozefowicz, R., Kaiser, L., Kudlur, M., Levenberg, J., Mane, D., Monga, R., Moore, S.,
662 Murray, D., Olah, C., Schuster, M., Shlens, J., Steiner, B., Sutskever, I., Talwar, K., Tucker,
663 P., Vanhoucke, V., Vasudevan, V., Viegas, F., Vinyals, O., Warden, P., Wattenberg, M.,
664 Wicke, M., Yu, Y., Zheng, X., 2016. TensorFlow: Large-Scale Machine Learning on
665 Heterogeneous Distributed Systems. <https://doi.org/10.48550/arXiv.1603.04467>
- 666 Addor, N., Newman, A.J., Mizukami, N., Clark, M.P., 2017. The CAMELS data set: catchment
667 attributes and meteorology for large-sample studies. *Hydrol Earth Syst Sci*.
668 <https://doi.org/10.5194/hess-21-5293-2017>



669 Amendola, M., Arcucci, R., Mottet, L., Casas, C.Q., Fan, S., Pain, C., Linden, P., Guo, Y.-K.,
670 2020. Data Assimilation in the Latent Space of a Neural Network.
671 <https://doi.org/10.48550/ARXIV.2012.12056>

672 Baydin, A.G., Pearlmutter, B.A., Radul, A.A., Siskind, J.M., 2018. Automatic differentiation in
673 machine learning: a survey. *J. Mach. Learn. Res.* 18, 1–43.

674 Blöschl, G., Bierkens, M.F.P., Chambel, A., Cudennec, C., Destouni, G., Fiori, A., Kirchner, J.W.,
675 McDonnell, J.J., Savenije, H.H.G., Sivapalan, M., Stumpp, C., Toth, E., Volpi, E., Carr, G.,
676 Lupton, C., Salinas, J., Széles, B., Viglione, A., Aksoy, H., Allen, S.T., Amin, A.,
677 Andréassian, V., Arheimer, B., Aryal, S.K., Baker, V., Bardsley, E., Barendrecht, M.H.,
678 Bartosova, A., Batelaan, O., Berghuijs, W.R., Beven, K., Blume, T., Bogaard, T., Borges De
679 Amorim, P., Böttcher, M.E., Boulet, G., Breinl, K., Brilly, M., Brocca, L., Buytaert, W.,
680 Castellarin, A., Castelletti, A., Chen, X., Chen, Yangbo, Chen, Yuanfang, Chifflard, P., Claps,
681 Clark, M.P., Collins, A.L., Croke, B., Dathe, A., David, P.C., De Barros, F.P.J., De Rooij,
682 Di Baldassarre, G., Driscoll, J.M., Duethmann, D., Dwivedi, R., Eris, E., Farmer, W.H.,
683 Feiccabruno, J., Ferguson, G., Ferrari, E., Ferraris, S., Fersch, B., Finger, D., Foglia, L.,
684 Fowler, K., Gartsman, B., Gascoin, S., Gaume, E., Gelfan, A., Geris, J., Gharari, S., Gleeson,
685 Glendell, M., Gonzalez Bevacqua, A., González-Dugo, M.P., Grimaldi, S., Gupta, A.B.,
686 Guse, B., Han, D., Hannah, D., Harpold, A., Haun, S., Heal, K., Helfricht, K., Herrnegger,
687 Hipsey, M., Hlaváčiková, H., Hohmann, C., Holko, L., Hopkinson, C., Hrachowitz, M.,
688 Illangasekare, T.H., Inam, A., Innocente, C., Istanbulluoglu, E., Jarihani, B., Kalantari, Z.,
689 Kalvans, A., Khanal, S., Khatami, S., Kiesel, J., Kirkby, M., Knoben, W., Kochanek, K.,
690 Kohnová, S., Kolechkina, A., Krause, S., Kreamer, D., Kreibich, H., Kunstmann, H., Lange,
691 Liberato, M.L.R., Lindquist, E., Link, T., Liu, J., Loucks, D.P., Luce, C., Mahé, G.,



- 692 Makarieva, O., Malard, J., Mashtayeva, S., Maskey, S., Mas-Pla, J., Mavrova-Guirguinova,
693 M., Mazzoleni, M., Mernild, S., Misstear, B.D., Montanari, A., Müller-Thomy, H.,
694 Nabizadeh, A., Nardi, F., Neale, C., Nesterova, N., Nurtaev, B., Odongo, V.O., Panda, S.,
695 Pande, S., Pang, Z., Papacharalampous, G., Perrin, C., Pfister, L., Pimentel, R., Polo, M.J.,
696 Post, D., Prieto Sierra, C., Ramos, M.-H., Renner, M., Reynolds, J.E., Ridolfi, E., Rigon, R.,
697 Riva, M., Robertson, D.E., Rosso, R., Roy, T., Sá, J.H.M., Salvadori, G., Sandells, M.,
698 Schaeffli, B., Schumann, A., Scolobig, A., Seibert, J., Servat, E., Shafiei, M., Sharma, A.,
699 Sidibe, M., Sidle, R.C., Skaugen, T., Smith, H., Spiessl, S.M., Stein, L., Steinsland, I., Strasser,
700 U., Su, B., Szolgay, J., Tarboton, D., Tauro, F., Thirel, G., Tian, F., Tong, R., Tussupova, K.,
701 Tyralis, H., Uijlenhoet, R., Van Beek, R., Van Der Ent, R.J., Van Der Ploeg, M., Van Loon,
702 A.F., Van Meerveld, I., Van Nooijen, R., Van Oel, P.R., Vidal, J.-P., Von Freyberg, J.,
703 Vorogushyn, S., Wachniew, P., Wade, A.J., Ward, P., Westerberg, I.K., White, C., Wood,
704 E.F., Woods, R., Xu, Z., Yilmaz, K.K., Zhang, Y., 2019. Twenty-three unsolved problems in
705 hydrology (UPH) – a community perspective. *Hydrol. Sci. J.* 64, 1141–1158.
706 <https://doi.org/10.1080/02626667.2019.1620507>
- 707 Brunner, M.I., Gilleland, E., Wood, A., Swain, D.L., Clark, M., 2020. Spatial Dependence of
708 Floods Shaped by Spatiotemporal Variations in Meteorological and Land-Surface Processes.
709 *Geophys. Res. Lett.* 47, e2020GL088000. <https://doi.org/10.1029/2020GL088000>
- 710 Budyko, M.I., Miller, D.H. (Eds.), 2010. Climate and life, International geophysics series.
711 Academic Press, New York.
- 712 Cho, K., Kim, Y., 2022. Improving streamflow prediction in the WRF-Hydro model with LSTM
713 networks. *J. Hydrol.* 605, 127297. <https://doi.org/10.1016/j.jhydrol.2021.127297>



- 714 Dembélé, M., Hrachowitz, M., Savenije, H.H.G., Mariéthoz, G., Schaefli, B., 2020. Improving the
715 Predictive Skill of a Distributed Hydrological Model by Calibration on Spatial Patterns With
716 Multiple Satellite Data Sets. *Water Resour. Res.* 56, e2019WR026085.
717 <https://doi.org/10.1029/2019WR026085>
- 718 Devitt, L., Neal, J., Coxon, G., Savage, J., Wagener, T., 2023. Flood hazard potential reveals global
719 floodplain settlement patterns. *Nat. Commun.* 14, 2801. [https://doi.org/10.1038/s41467-023-38297-9](https://doi.org/10.1038/s41467-023-
720 38297-9)
- 721 Dong, Z., Hu, H., Liu, H., Baiyin, B., Mu, X., Wen, J., Liu, D., Chen, L., Ming, G., Chen, X., Li,
722 X., 2024. Superior performance of hybrid model in ungauged basins for real-time hourly
723 water level forecasting – A case study on the Lancang-Mekong mainstream. *J. Hydrol.* 633,
724 130941. <https://doi.org/10.1016/j.jhydrol.2024.130941>
- 725 Fang, K., Kifer, D., Lawson, K., Feng, D., Shen, C., 2022. The Data Synergy Effects of Time-
726 Series Deep Learning Models in Hydrology. *Water Resour. Res.* 58, e2021WR029583.
727 <https://doi.org/10.1029/2021WR029583>
- 728 Fang, K., Shen, C., Kifer, D., Yang, X., 2017. Prolongation of SMAP to Spatiotemporally
729 Seamless Coverage of Continental U.S. Using a Deep Learning Neural Network. *Geophys.
730 Res. Lett.* 44. <https://doi.org/10.1002/2017GL075619>
- 731 Feng, D., Fang, K., Shen, C., 2020. Enhancing Streamflow Forecast and Extracting Insights Using
732 Long-Short Term Memory Networks With Data Integration at Continental Scales. *Water
733 Resour. Res.* 56, e2019WR026793. <https://doi.org/10.1029/2019WR026793>
- 734 Frame, J.M., Kratzert, F., Raney, A., Rahman, M., Salas, F.R., Nearing, G.S., 2021. Post-
735 Processing the National Water Model with Long Short-Term Memory Networks for



- 736 Streamflow Predictions and Model Diagnostics. *JAWRA J. Am. Water Resour. Assoc.* 57,
737 885–905. <https://doi.org/10.1111/1752-1688.12964>
- 738 Gao, X.J., Wang, M.L., Filippo, G., 2013. Climate change over China in the 21st century as
739 simulated by BCC_CSM1. 1-RegCM4.0. *Atmos. Oceanic Sci. Lett.* 6 (5), 381–386.
740 <https://doi.org/10.3878/j.issn.1674-2834.13.0029>
- 741 Herrera, P.A., Marazuela, M.A., Hofmann, T., 2022. Parameter estimation and uncertainty analysis
742 in hydrological modeling. *WIREs Water* 9, e1569. <https://doi.org/10.1002/wat2.1569>
- 743 Hersbach, H., Bell, B., Berrisford, P., Hirahara, S., Horányi, A., Muñoz-Sabater, J., Nicolas, J.,
744 Peubey, C., Radu, R., Schepers, D., Simmons, A., Soci, C., Abdalla, S., Abellán, X., Balsamo,
745 Bechtold, P., Biavati, G., Bidlot, J., Bonavita, M., De Chiara, G., Dahlgren, P., Dee, D.,
746 Diamantakis, M., Dragani, R., Flemming, J., Forbes, R., Fuentes, M., Geer, A., Haimberger,
747 Healy, S., Hogan, R.J., Hólm, E., Janisková, M., Keeley, S., Laloyaux, P., Lopez, P., Lupu,
748 Radnoti, G., De Rosnay, P., Rozum, I., Vamborg, F., Villaume, S., Thépaut, J., 2020. The
749 ERA5 global reanalysis. *Q. J. R. Meteorol. Soc.* 146, 1999–2049.
750 <https://doi.org/10.1002/qj.3803>
- 751 Hochreiter, S., Schmidhuber, J., 1997. Long Short-Term Memory. *Neural Comput.* 9, 1735–1780.
752 <https://doi.org/10.1162/neco.1997.9.8.1735>
- 753 Höge, M., Scheidegger, A., Baity-Jesi, M., Albert, C., Fenicia, F., 2022. Improving hydrologic
754 models for predictions and process understanding using neural ODEs. *Hydrol. Earth Syst. Sci.*
755 26, 5085–5102. <https://doi.org/10.5194/hess-26-5085-2022>
- 756 Hoy, A.Q., 2017. Protecting water resources calls for internationalefforts. *Science* 356, 814–815.
757 <https://doi.org/10.1126/science.356.6340.814>



- 758 Hrachowitz, M., Savenije, H., Blöschl, G., McDonnell, J., Sivapalan, M., Pomeroy, J., et al. (2013).
759 A decade of Predictions in Ungauged Basins (PUB)—A review. *Hydrological sciences*
760 journal, 58(6), 1198–1255.
- 761 Innes, M., 2018. Flux: Elegant machine learning with Julia. *J. Open Source Softw.* 3, 602.
762 <https://doi.org/10.21105/joss.00602>
- 763 Jiang, S., Zheng, Y., Solomatine, D., 2020. Improving AI System Awareness of Geoscience
764 Knowledge: Symbiotic Integration of Physical Approaches and Deep Learning. *Geophys. Res.*
765 Lett.
- 766 Jiao, D., Xu, N., Yang, F., Xu, K., 2021. Evaluation of spatial-temporal variation performance of
767 ERA5 precipitation data in China. *Sci. Rep.* 11, 17956. <https://doi.org/10.1038/s41598-021-97432-y>
- 769 Karp, R.M., Miller, R.E., 1966. Properties of a Model for Parallel Computations: Determinacy,
770 Termination, Queueing. *SIAM J. Appl. Math.* 14, 1390–1411.
771 <https://doi.org/10.1137/0114108>
- 772 Kim, Y.W., Kim, T., Shin, J., Go, B., Lee, M., Lee, J., Koo, J., Cho, K.H., Cha, Y., 2021.
773 Forecasting Abrupt Depletion of Dissolved Oxygen in Urban Streams Using Discontinuously
774 Measured Hourly Time-Series Data. *Water Resour. Res.* 57, e2020WR029188.
775 <https://doi.org/10.1029/2020WR029188>
- 776 Kingma, D.P., Ba, J., 2014. Adam: A Method for Stochastic Optimization.
777 <https://doi.org/10.48550/ARXIV.1412.6980>



- 778 Knoben, W.J.M., Freer, J.E., Woods, R.A., 2019. Technical note: Inherent benchmark or not?
- 779 Comparing Nash–Sutcliffe and Kling–Gupta efficiency scores. *Hydrol. Earth Syst. Sci.* 23,
- 780 4323–4331. <https://doi.org/10.5194/hess-23-4323-2019>
- 781 Koch, J., Cornelissen, T., Fang, Z., Bogena, H., Diekkrüger, B., Kollet, S., Stisen, S., 2016. Inter-
782 comparison of three distributed hydrological models with respect to seasonal variability of
783 soil moisture patterns at a small forested catchment. *J. Hydrol.* 533, 234–249.
784 <https://doi.org/10.1016/j.jhydrol.2015.12.002>
- 785 Konapala, G., Kao, S.-C., Painter, S.L., Lu, D., 2020. Machine learning assisted hybrid models
786 can improve streamflow simulation in diverse catchments across the conterminous US.
787 *Environ. Res. Lett.* 15, 104022. <https://doi.org/10.1088/1748-9326/aba927>
- 788 Kratzert, F., Klotz, D., Brenner, C., Schulz, K., Herrnegger, M., 2018. Rainfall–runoff modelling
789 using Long Short-Term Memory (LSTM) networks. *Hydrol. Earth Syst. Sci.* 22, 6005–6022.
790 <https://doi.org/10.5194/hess-22-6005-2018>
- 791 Kratzert, F., Klotz, D., Herrnegger, M., Sampson, A.K., Hochreiter, S., Nearing, G.S., 2019a.
792 Toward Improved Predictions in Ungauged Basins: Exploiting the Power of Machine
793 Learning. *Water Resour. Res.* 55, 11344–11354. <https://doi.org/10.1029/2019WR026065>
- 794 Kratzert, F., Klotz, D., Shalev, G., Klambauer, G., Hochreiter, S., Nearing, G., 2019b. Towards
795 learning universal, regional, and local hydrological behaviors via machine learning applied
796 to large-sample datasets. *Hydrol. Earth Syst. Sci.* 23, 5089–5110.
797 <https://doi.org/10.5194/hess-23-5089-2019>
- 798 Kratzert, F., Nearing, G., Addor, N., Erickson, T., Gauch, M., Gilon, O., Gudmundsson, L.,
799 Hassidim, A., Klotz, D., Nevo, S., Shalev, G., Matias, Y., 2023. Caravan - A global



800 community dataset for large-sample hydrology. Sci. Data 10, 61.

801 <https://doi.org/10.1038/s41597-023-01975-w>

802 Lehner, B., Verdin, K., Jarvis, A., 2008. New Global Hydrography Derived From Spaceborne

803 Elevation Data. Eos Trans. Am. Geophys. Union 89, 93–94.

804 <https://doi.org/10.1029/2008EO100001>

805 Li, B., Sun, T., Tian, F., Ni, G., 2023. Enhancing process-based hydrological models with

806 embedded neural networks: A hybrid approach. J. Hydrol. 625, 130107.

807 <https://doi.org/10.1016/j.jhydrol.2023.130107>

808 Liang, X., Lettenmaier, D.P., Wood, E.F., Burges, S.J., 1994. A simple hydrologically based model

809 of land surface water and energy fluxes for general circulation models. J. Geophys. Res.

810 Atmospheres 99, 14415–14428. <https://doi.org/10.1029/94JD00483>

811 Liu, J., Rahmani, F., Lawson, K., Shen, C., 2022. A Multiscale Deep Learning Model for Soil

812 Moisture Integrating Satellite and In Situ Data. Geophys. Res. Lett. 49, e2021GL096847.

813 <https://doi.org/10.1029/2021GL096847>

814 Liu, R., Zhang, X., Wang, W., Wang, Y., Liu, H., Ma, M., Tang, G., 2024. Global-scale ERA5

815 product precipitation and temperature evaluation. Ecol. Indic. 166, 112481.

816 <https://doi.org/10.1016/j.ecolind.2024.112481>

817 Liu, X., Zhang, L., She, D., Chen, J., Xia, J., Chen, X., Zhao, T., 2022. Postprocessing of

818 hydrometeorological ensemble forecasts based on multisource precipitation in Ganjiang

819 River basin, China. J. Hydrol. 605, 127323. <https://doi.org/10.1016/j.jhydrol.2021.127323>



- 820 Mangukiya, N.K., Sharma, A., 2025. Deep Learning-Based Approach for Enhancing Streamflow
821 Prediction in Watersheds With Aggregated and Intermittent Observations. *Water Resour. Res.*
822 61, e2024WR037331. <https://doi.org/10.1029/2024WR037331>
- 823 Mangukiya, N.K., Yadav, S.M., 2022. Integrating 1D and 2D hydrodynamic models for semi-arid
824 river basin flood simulation. *Int. J. Hydrol. Sci. Technol.* 14, 206.
825 <https://doi.org/10.1504/IJHST.2022.124549>
- 826 Meng Xianyong, Wang Hao, Lei Xiaohui, Cai Siyu, 2017. Simulation, validation, and analysis of
827 the Hydrological components of Jing and Bo River Basin based on the SWAT model driven
828 by CMADS. *Acta Ecol. Sin.* 37. <https://doi.org/10.5846/stxb201608231719>
- 829 Miao, Y., Wang, A., 2020. A daily $0.25^\circ \times 0.25^\circ$ hydrologically based land surface flux dataset
830 for conterminous China, 1961–2017. *J. Hydrol.* 590, 125413.
831 <https://doi.org/10.1016/j.jhydrol.2020.125413>
- 832 Newman, A.J., Clark, M.P., Sampson, K., Wood, A., Hay, L.E., Bock, A., Viger, R.J., Blodgett,
833 Brekke, L., Arnold, J.R., Hopson, T., Duan, Q., 2015. Development of a large-sample
834 watershed-scale hydrometeorological data set for the contiguous USA: data set characteristics
835 and assessment of regional variability in hydrologic model performance. *Hydrol. Earth Syst.
836 Sci.* 19, 209–223. <https://doi.org/10.5194/hess-19-209-2015>
- 837 O., S., Orth, R., 2021. Global soil moisture data derived through machine learning trained with in-
838 situ measurements. *Sci. Data* 8, 170. <https://doi.org/10.1038/s41597-021-00964-1>
- 839 Paszke, A., Gross, S., Massa, F., Lerer, A., Bradbury, J., Chanan, G., Killeen, T., Lin, Z.,
840 Gimelshein, N., Antiga, L., Desmaison, A., Köpf, A., Yang, E., DeVito, Z., Raison, M.,
841 Tejani, A., Chilamkurthy, S., Steiner, B., Fang, L., Bai, J., Chintala, S., 2019. PyTorch: An



842 Imperative Style, High-Performance Deep Learning Library.

843 <https://doi.org/10.48550/arXiv.1912.01703>

844 Patil, S., Stieglitz, M., 2014. Modelling daily streamflow at ungauged catchments: what
845 information is necessary?: MODELLING DAILY STREAMFLOW AT UNGAUGED
846 CATCHMENTS. *Hydrol. Process.* 28, 1159–1169. <https://doi.org/10.1002/hyp.9660>

847 Patle, P., Sharma, A., 2023. Evaluation of Water Resources in a Complex River Basin Using Water
848 Accounting Plus: A Case Study of the Mahi River Basin in India. *J. Water Resour. Plan.*
849 *Manag.* 149, 05023017. <https://doi.org/10.1061/JWRMD5.WRENG-6125>

850 Qiu, R., Wang, Y., Rhoads, B., Wang, D., Qiu, W., Tao, Y., Wu, J., 2021. River water temperature
851 forecasting using a deep learning method. *J. Hydrol.* 595, 126016.
852 <https://doi.org/10.1016/j.jhydrol.2021.126016>

853 Rahmani, F., Appling, A., Feng, D., Lawson, K., Shen, C., 2023. Identifying Structural Priors in a
854 Hybrid Differentiable Model for Stream Water Temperature Modeling. *Water Resour. Res.*
855 59, e2023WR034420. <https://doi.org/10.1029/2023WR034420>

856 Ren-Jun, Z., 1992. The Xinanjiang model applied in China. *J. Hydrol.* 135, 371–381.
857 [https://doi.org/10.1016/0022-1694\(92\)90096-E](https://doi.org/10.1016/0022-1694(92)90096-E)

858 Satoh, Y., Yoshimura, K., Pokhrel, Y., Kim, H., Shiogama, H., Yokohata, T., Hanasaki, N., Wada,
859 Y., Burek, P., Byers, E., Schmied, H.M., Gerten, D., Ostberg, S., Gosling, S.N., Boulange,
860 J.E.S., Oki, T., 2022. The timing of unprecedented hydrological drought under climate change.
861 *Nat. Commun.* 13, 3287. <https://doi.org/10.1038/s41467-022-30729-2>

862 Shen, Y., Ruijsch, J., Lu, M., Sutanudjaja, E.H., Karssenberg, D., 2022. Random forests-based
863 error-correction of streamflow from a large-scale hydrological model: Using model state



864 variables to estimate error terms. Comput. Geosci. 159, 105019.

865 <https://doi.org/10.1016/j.cageo.2021.105019>

866 Silvestro, F., Gabellani, S., Rudari, R., Delogu, F., Laiolo, P., Boni, G., 2015. Uncertainty
867 reduction and parameter estimation of a distributed hydrological model with ground and
868 remote-sensing data. Hydrol. Earth Syst. Sci. 19, 1727–1751. <https://doi.org/10.5194/hess-19-1727-2015>

870 Sivapalan, M., Takeuchi, K., Franks, S., Gupta, V., Karambiri, H., Lakshmi, V., et al. (2003).
871 IAHS decade on Predictions in Ungauged Basins (PUB), 2003–2012: Shaping an exciting
872 future for the hydrological sciences. Hydrological sciences journal, 48(6), 857–880.

873 Slater, L.J., Arnal, L., Boucher, M.-A., Chang, A.Y.-Y., Moulds, S., Murphy, C., Nearing, G.,
874 Shalev, G., Shen, C., Speight, L., Villarini, G., Wilby, R.L., Wood, A., Zappa, M., 2023.
875 Hybrid forecasting: blending climate predictions with AI models. Hydrol. Earth Syst. Sci. 27,
876 1865–1889. <https://doi.org/10.5194/hess-27-1865-2023>

877 Tan, Xuejin, Liu, B., Tan, Xuezhi, Chen, X., 2022. Long-Term Water Imbalances of Watersheds
878 Resulting From Biases in Hydroclimatic Data Sets for Water Budget Analyses. Water Resour.
879 Res. 58, e2021WR031209. <https://doi.org/10.1029/2021WR031209>

880 Tsai, W.-P., Feng, D., Pan, M., Beck, H., Lawson, K., Yang, Y., Liu, J., Shen, C., 2021. From
881 calibration to parameter learning: Harnessing the scaling effects of big data in geoscientific
882 modeling. Nat. Commun. 12, 5988. <https://doi.org/10.1038/s41467-021-26107-z>

883 Wang, S., Huang, J., Li, J., Rivera, A., McKenney, D.W., Sheffield, J., 2014. Assessment of water
884 budget for sixteen large drainage basins in Canada. J. Hydrol. 512, 1–15.
885 <https://doi.org/10.1016/j.jhydrol.2014.02.058>



- 886 Wang, Y., Liu, J., Li, C., Liu, Y., Xu, L., Yu, F., 2023. A data-driven approach for flood prediction
887 using grid-based meteorological data. *Hydrol. Process.* 37, e14837.
888 <https://doi.org/10.1002/hyp.14837>
- 889 Willard, J.D., Read, J.S., Appling, A.P., Oliver, S.K., Jia, X., Kumar, V., 2021. Predicting Water
890 Temperature Dynamics of Unmonitored Lakes With Meta-Transfer Learning. *Water Resour.*
891 *Res.* 57, e2021WR029579. <https://doi.org/10.1029/2021WR029579>
- 892 Wu, M., Liu, P., Liu, L., Zou, K., Luo, X., Wang, J., Xia, Q., Wang, H., 2024. Improving a
893 hydrological model by coupling it with an LSTM water use forecasting model. *J. Hydrol.* 636,
894 131215. <https://doi.org/10.1016/j.jhydrol.2024.131215>
- 895 Xu, Y., Lin, K., Hu, C., Wang, S., Wu, Q., Zhang, L., Ran, G., 2023. Deep transfer learning based
896 on transformer for flood forecasting in data-sparse basins. *J. Hydrol.* 625, 129956.
897 <https://doi.org/10.1016/j.jhydrol.2023.129956>
- 898 Yin, Z., Ottlé, C., Ciais, P., Guimbertea, M., Wang, X., Zhu, D., Maignan, F., Peng, S., Piao, S.,
899 Polcher, J., Zhou, F., Kim, H., other China-Trend-Stream project members, 2018. Evaluation
900 of ORCHIDEE-MICT-simulated soil moisture over China and impacts of different
901 atmospheric forcing data. *Hydrol. Earth Syst. Sci.* 22, 5463–5484.
902 <https://doi.org/10.5194/hess-22-5463-2018>
- 903 Zhang, B., Ouyang, C., Cui, P., Xu, Q., Wang, D., Zhang, F., Li, Z., Fan, L., Lovati, M., Liu, Y.,
904 Zhang, Q., 2024. Deep learning for cross-region streamflow and flood forecasting at a global
905 scale. *The Innovation* 5, 100617. <https://doi.org/10.1016/j.xinn.2024.100617>
- 906 Zhi, W., Feng, D., Tsai, W.-P., Sterle, G., Harpold, A., Shen, C., Li, L., 2021. From
907 Hydrometeorology to River Water Quality: Can a Deep Learning Model Predict Dissolved



908 Oxygen at the Continental Scale? Environ. Sci. Technol. 55, 2357–2368.

909 <https://doi.org/10.1021/acs.est.0c06783>

910